Structure and function of the human periodontium

Science meets the clinician

Azaripour, A.

Publication date
2016
Document Version
Other version
License
Other

Chapter 3

Three-dimensional imaging of human gingiva

Three-dimensional histochemistry and imaging of human gingiva

Adriano Azaripour[1, 2], Tonny Lagerweij[3], Christina Scharfbillig[1], Anna Elisabeth Jadczak[1], Wikky Tigchelaar[2], Daisy I. Picavet[2], Esther M.L. Hendrikx[4], Cornelis J.F. Van Noorden[2]

1) Department of Operative Dentistry, University Medical Center of the Johannes Gutenberg University Mainz, Augustusplatz 2, Mainz 55131, Germany
2) Department of Cell Biology and Histology, Academic Medical Center, University of Amsterdam, Amsterdam, The Netherlands
3) Neuro-oncology Research Group, VU University Medical Center, Cancer Center Amsterdam, Room 3.56, De Boelelaan 1117, 1081 HV Amsterdam, The Netherlands
4) Molecular Cell Biology and Immunology, VU University Medical Center, De Boelelaan 1117, 1081 HV Amsterdam, The Netherlands

Correspondence:
Dr. Adriano Azaripour
Department of Operative Dentistry, University Medical Center of the Johannes Gutenberg University Mainz, Augustusplatz 2, Mainz 55131, Germany
e-mail: adrianoasso@hotmail.com

Conflict of interest and source funding statement: The authors declare that they have no conflict of interests. No funding from sources has to be reported.

Abstract

Aim: To develop 3D histochemistry and imaging methodology for human gingiva to analyze its vasculature.

Materials and Methods: Nine human gingiva samples without signs of inflammation were cleared using a mixture of 2 part benzyl benzoate and 1 part benzyl alcohol (BABB), stained for CD 31, a marker of endothelium, using immunofluorescence in combination with YOYO-3, a fluorescent DNA dye, imaged with the use of light-sheet microscopy and image processing with Imaris software.

Results: 3D images showed the vascular network in the lamina propria of gingiva with loops into the gingiva papillae of the lamina propria. The vascular network in these human gingivas showed a high degree of tortuosity and irregularities in structure which are not apparent in images of sections of gingiva.

Conclusions: The 3D histochemistry and imaging methodology described here is a promising novel approach to study structural aspects of human gingiva that are involved in diseased periodontium.

Keywords: Tissue clearing, extracellular matrix, histology, gingiva, connective tissue, microscopy

Introduction

Traditional 2D histological assessment of tissues limits proper insights in 3D tissue structure. Imaging of serial sections of a tissue and subsequent 3D reconstruction of the tissue on the basis of those images have been performed successfully (Griffini et al., 1997), but its application has remained limited to small volumes of tissue and it is a time-consuming and error-prone procedure (Peng et al., 2014; Chieco et al., 2013; Chung et al., 2013; Griffini et al., 1997). 3D imaging of tissues is hampered by the fact that tissues are opaque which limits imaging to a depth of 500-1000 μm at best (Weigelin et al., 2016). Opaqueness of tissues is mainly caused by cell membranes (Chung et al., 2013) and extracellular matrix (ECM; Azaripour et al., 2016). Therefore, a tissue-clearing step has to be included for 3D imaging of tissues.

The German anatomist Werner Spalteholz (1861–1940; Spalteholz, 1911, 1914) was the first scientist who investigated clearing of tissues. For the 3D study of anastomoses between coronary arteries in the heart, he developed a solution with ideal chemical characteristics for tissue clearing. The solution consisted of methyl salicylate, benzyl benzoate (BB) and wintergreen oil. Opaqueness of tissues is based on different refractive indices (RIs) of tissues and their environment such as embedding medium, cover glass and microscopic slide. Spalteholz (1911, 1914) discovered that when the RI of the embedding or clearing medium was too high, tissue was not transparent and when it was too low, refraction and reflection of light occurred at the surface of tissues. His clearing medium prevented that. However, what he did not prevent was tissue shrinkage (Hama et al., 2011; Ke et al., 2013), the formation of bubbles due to the effect of hydrogen peroxide what he used for bleaching of endogenous pigments (Cumley et al., 1939) and the occurrence of necrosis in the outer layer of tissue samples (Steinke and Wolff, 2001).

Recently, 3D histochemistry was introduced as an important novel development (Dodt et al., 2007; Chung et al., 2013). In particular, novel methods to clear tissues were reported (for review, see Azaripour et al. 2016). However, most of these methods are focused on the central nervous system and embryos. Opacity of these tissues is mainly caused by lipid bilayers of cell membranes and not by ECM, because these tissues contain only small amounts of connective tissue. Therefore, the novel clearing methods are focused on the removal of lipid bilayers of cell membranes (Hama et al., 2011; Kuwajima et al., 2013; Ke et al., 2013; Susaki

et al., 2014; Chung et al., 2013; Yang et al., 2014; Lee et al., 2016) rather than the clearing of ECM. Clearing of ECM-rich tissues such as skin or gingiva need an alternative approach (Dodt et al., 2007; Erturk et al., 2012; Renier et al., 2014).

The aim of the present study was to investigate the possibilities of 3D imaging of blood vessels in gingiva. 3D histochemistry and imaging allow the visualization of various tissue structures in relation to each other, which is important to understand structure and function of tissues (Nuki and Hock, 1975; Fujimura and Nozaka, 2002). The anatomy of the gingival vasculature is known (Lindhe et al., 2008), but studies are not available at the cellular level. Furthermore, investigations have usually been performed on gingiva of animals. For these investigations, vessels are usually perfused using plastic monomers, gelatin, silicone or latex that are polymerized or solidified afterwards (Egelberg, 1966; Lindhe et al., 2008). Next, the tissue is macerated, hydrolyzed or removed and only the vasculature with the solidified content remains (Draenert and Draenert, 1980). The present study describes our investigations to optimize clearing and imaging of human gingiva using the benzyl alcohol (BA) and BB-containing clearing solution BABB and light-sheet microscopy.

Materials and Methods

Experiments were performed on 9 samples of human gingiva that were acquired as waste patient material during periodontal surgery or tooth extraction at the Department of Operative Dentistry and Periodontology of the University of Mainz, Germany. The samples did not show signs of inflammation such as swelling, redness or bleeding. Patients were healthy and between 40 and 60 years old. Patients were informed about the aim of the study and signed an informed consent document. After removal, samples were stored in freshly-prepared 4% paraformaldehyde (PFA; Merck, Darmstadt, Germany) in phosphate-buffered saline (PBS; pH 7.2; Gibco Life Technologies, Carlsbad, CA, USA). All experiments were performed in the Department of Cell Biology and Histology of the Academic Medical Centre (AMC) at the University of Amsterdam, The Netherlands.

Preparation of gingiva samples

The first preparation steps of the gingiva samples were performed under gentle but constant shaking. Each incubation step lasted 60 min at room temp unless stated otherwise. Samples were removed from the PFA solution and were washed twice in PBS. Afterwards, samples were dehydrated in an ascending series of methanol in PBS (50%, 80%, 100%) and finally stored in 100% methanol overnight at room temp. Bleaching of the gingiva samples to reduce autofluorescence (Renier et al., 2014) was performed at 4°C overnight in a solution containing 1 part 30% H_2O_2 (Merck) 1 part DMSO (Merck) and 4 parts ice-cold methanol. Bleaching solution was replaced 3 times by 100% methanol and then twice by 20% DMSO in methanol. Finally, gingiva samples were rehydrated in a descending methanol series in PBS (80%, 50%, 0%) and were stored as briefly as possible in PBS at room temp containing 0.1% Triton X-100 (Sigma-Aldrich, St. Louis, MO, USA) until staining was applied.

Staining of gingiva

Gingiva samples were stained with a cocktail containing anti-CD31 antibodies (clone EN4; Monosan, Sanbio, Uden, The Netherlands) conjugated with Alexa Fluor® 568 (Life Technologies; dilution, 1:100) as general human endothelial cell marker (Hira et al., 2015) and YOYO-3 (Life Technologies) in a 1:5000 dilution for nuclear staining. Samples were stained at room temp for 7 days.

Clearing of gingiva

Gingiva samples were washed after staining using PBS containing 0.2% Tween 20 (Sigma-Aldrich) for 4 times at room temp. Gingiva samples were then embedded in 2% NuSieve GTG low-melting temp agarose (Lonza, Basel, Switzerland) to facilitate handling in the microscope (Fig. 1). Samples were treated with a series of methanol in distilled water starting at 50% methanol, then followed by 70%, 80%, 96% and 3 times 100% methanol. Next, a mixture of 50% methanol and 50% BABB (BA and BB both from Sigma-Aldrich) was used for tissue storage overnight at room temp. The following morning, the methanol/BABB mixture was replaced by 100% BABB, the final clearing solution, and the samples were stored in 100% BABB.

Imaging of gingiva

Gingiva samples were imaged using light-sheet microscopy (LaVision BioTec, Bielefeld, Germany) with a x10 MVX objective (Olympus, Tokyo, Japan). As DBE is generally used as imaging medium for light-sheet microscopy and because the RIs of BABB and DBE are similar, BABB was replaced with DBE (Sigma-Aldrich) as imaging medium. Alexa Fluor ® 568 was excited at 578 nm whereas emission was detected at 603 nm and YOYO-3 was excited at 612 nm whereas emission was detected at 631 nm. 3D images were taken in approx. 15 min.

Image processing

To process the data sets, Imaris x64 7.4.2 software (Bitplane, Belfast, UK) was used.

Results

Clearing and staining of gingiva

Gingiva samples cleared with BABB became transparent within 4 h. Fig. 1 shows untreated opaque gingiva and cleared gingiva in BABB. Embedding of the gingiva samples in agarose, as is shown in Fig. 1, made handling of the samples for light-sheet microscopy easy. Optimal staining with antibodies lasted 6 days at room temp. Nuclear staining with YOYO-3 needed only a few hours. However, addition of yoyo-3 to the antibodies-containing incubation medium in a 1:5000 dilution appeared to be the best approach. Thus, the process from dissecting gingiva in a patient up to visualization of the specimen in a light-sheet microscope lasted approx. a week.

Imaging of gingiva

In pilot experiments, confocal laser scanning microscopy and light-sheet microscopy were compared for their use in 3D histochemistry and imaging of human gingiva. First, from a practical point of view was light-sheet microscopy superior because the hydrophobic imaging medium (BABB or DBE) caused damage to the confocal microscope whereas the special tissue holders of the light-sheet microscope are resistant against BABB and DBE. Second, the tissue volume that can be imaged with light-sheet microscopy (1 mm^3-5000 mm^3) with a spatial resolution up to 1µm appeared to be by far larger than the tissue volumes that a confocal microscope can handle. Third, imaging with light-sheet microscopy was considerably faster than that with a confocal microscope. Imaging of the gingiva samples needed less than an hour when using light-sheet microscopy and an entire night when using confocal microscopy. Fourth, out-of-focus excitation did not play a significant role in light-sheet microscopy, whereas it did in confocal microscopy (Hoebe et al., 2007). Out-of-focus excitation is a major cause of photobleaching and photodamage (Hoebe et al. 2007). Therefore, light-sheet microscopy was selected as the imaging technique of choice for all further experiments.

Images of gingiva

Figs 2-4 show 2D projections of 3D images obtained from human gingiva using ligh-sheet microscopy at various magnifications. The Suppl. Movie shows an image in 3D. All images show vasculature in the lamina propria of gingiva. Because the blood vessels are stained by demonstrating CD-31 which is a marker of endothelium, arterioles, capillaries and venules

cannot be discriminated. A remarkable phenomenon of the vascular network in human gingiva was the tortuosity of the vessels and the large amount of morphological irregularities. This was a surprising finding because all gingivas had been obtained from healthy patients without any sign of gingival inflammation. In the present study, we focused on the capillary loops in papillae of the lamina propria underneath the multilayered epithelium (Fig. 4). In each papilla such a loop was found.

Discussion

In the present study, 3D images of blood vessels in human gingiva are presented for the first time after clearing gingiva with BABB and imaging of gingiva immersed in DBE with the use of light-sheet microcopy. This method opens new avenues to investigate the 3D structure of blood vessels in gingiva and its pathological variations due to, for example, smoking or diabetes. Quantitative evaluation of blood vessels and determination of changes in diameter of the blood vessels are possible using 3D histology with the use of image analysis (Wu et al., 2014; Peng et al., 2014; Chieco et al., 2013; Wesseling et al., 1994).

Orban (1948) emphasized the importance of histological investigations of gingival structures as basis of comprehensive clinical interpretation and understanding of its disorders. However, most studies investigating morphological changes in gingival blood vessels have been performed in animal models after perfusion using India Ink (Söderholm and Egelberg, 1973). The authors explored early vascular changes during the development of gingivitis in dogs, and differences in topography of the vascular system around teeth and implants have also been studied in animals (Berglundh et al. 1994). Richly-vascularized supracrestal connective tissue was found around teeth whereas supracrestal connective tissue around implants virtually lacked vascularization. The application of scanning electron microscopy enabled detailed imaging of the vascular network of gingiva and periodontal ligament cells in animal models (Matsuo and Takahashi, 2002). Effects of poor oral hygiene on gingiva have been imaged in vivo using confocal microscopy in humans (Eberhard et al., 2014). Animal studies are still necessary to study pathological processes in tissues when these cannot be studied in humans. However, animal studies for clinical investigations have to be limited as much as possible (Grafström et al., 2015). First, human and animal tissues are different in many biologically-relevant aspects and evaluation and interpretation of animal studies in the light of human pathology often goes wrong (e.g. Atai et al., 2011). Second, restriction of the numbers of animals used in scientific research is a major moral and political issue and therefore alternatives for animal experiments should be preferred. The present 3D histochemistry and imaging technology promises to be an excellent tool to acquire insights in human gingival morphology and vascular structures using waste patient material. It is an easy and cheap procedure and except for light-sheet microcopy, no specialized or expensive equipment is needed. Moreover, light-sheet microscopy is becoming more and more routinely-used equipment in histology (Icha et al., 2016). The preparation of tissues for 3D histochemistry

and imaging is relatively fast with a clearing procedure of 1-4 h and immunohistochemical staining for a week, whereas fluorescence signals are well-preserved and quenching does not occur. An unwanted effect of BABB clearing is tissue shrinkage. Twenty percent shrinkage is caused by BABB clearing (Parra et al., 2012; Vesuna et al., 2011). The extent of shrinkage depends on the dehydration procedures. The faster dehydration is performed, the more shrinkage occurs, so it is advised to dehydrate slowly (Erturk et al., 2012).

There are various clinical issues that can be addressed using 3D histochemistry and imaging. It is well known that diabetic patients develop novel leaky blood vessels in retina (Klaassen et al., 2015; Wong et al., 2016). However, only a few studies report what the effect of diabetes are on gingival microvaculature. Keene (1969) performed a histological investigation in diabetic patients using samples of the non-inflamed palatal gingiva. An increased periodic acid-Schiff (PAS)-positive staining was observed in diabetic gingival blood vessels indicating a thickening of the basal lamina in the blood vessel walls (Schultz-Haudt et al., 1961). Furthermore, the effects of aging on gingival blood vessels can be explored perfectly well with 3D histochemistry and imaging. Aging effects on human gingival vascular function have been reported by Matheny et al. (1993) using laser Doppler flowmetry. Laser Doppler flowmetry is a non-invasive method that has been used to evaluate the gingival blood flow in health and diseases (Ambrosini et al., 2002) or blood flow changes in smokers (Baab and Ödeberg, 1987) and after periodontal surgery (Retzepi et al., 2007). However, this methodology as well as dark field imaging (Donati et al., 2013; Sorelli et al., 2015) do not allow the analysis of blood vessel morphology in relation to surrounding tissues (the microenvironment) as it images the blood flow only.

Smoking is related to gingivitis, periodontitis and epithelial malignancy (Jalayeri Naderi et al., 2015). Smokers show a 4 times higher risk to acquire periodontitis in comparison to persons that never smoked (Tomar and Asma, 2000). However, studies have reported contrasting results and the mechanisms of how smoking affect periodontium are still unclear (Van Dyke and Dave, 2005). 3D histochemistry and imaging of gingiva may well become a useful novel approach to elucidate causes of physiological and pathological changes in human gingiva in a similar manner as occurs in the retina with the use of ophthalmic imaging which can be performed in vivo and non-invasively because the eye is transparent (Ramos de Carvalho et al., 2014). It is expected that 3D histochemistry of gingiva as is outlined in the present study will allow similar progress in the understanding of diseases in gingiva.

For future research on the vascular network in the lamina propria of gingiva, we will focus on the capillary loops in the papillae because they are essential for the viability of the epithelium. We hypothesize that especially these loops are vulnerable in conditions such as diabetes and smoking which has, no doubt, serious implications for the health of the epithelium.

References:

Ambrosini P, Cherene S, Miller N, Weissenbach M, Penaud J (2002). A laser Doppler study of gingival blood flow variations following periosteal stimulation. *J. Clin. Periodontol.* 29:103–7.

Atai NA, Renkema-Mills NA, Bosman J, Schmidt N, Rijkeboer D, Tigchelaar W, et al. (2011). Differential activity of NADPH-producing dehydrogenases renders rodents unsuitable models to study IDH1R132 mutation effects in human glioblastoma. *J. Histochem. Cytochem.* 59:489–503.

Azaripour A, Lagerweij T, Scharfbillig C, Jadczak AE, Willershausen B, Van Noorden CJF (2016). A survey of clearing techniques for 3D imaging of tissues with special reference to connective tissue. *Prog. Histochem. Cytochem.*51:9-23

Baab DA, Ödeberg PA (1987). The effect of cigarette smoking on gingival blood flow in humans. *J. Periodontol.* 14:418–424.

Berglundh T, Lindhe J, Jonsson K, Ericsson I (1994). The topography of the vascular systems in the periodontal and peri-implant tissues in the dog. *J. Clin. Periodontol.* 21:189–193.

Chieco P, Jonker A, De Boer BA, Ruijter JM, Van Noorden CJF (2013). Image cytometry: protocols for 2D and 3D quantification in microscopic images. *Prog. Histochem. Cytochem.* 47:211-333.

Chung K, Wallace J, Kim SY, Kalyanasundaram S, Andalman AS, Davidson TJ, et al. (2013). Structural and molecular interrogation of intact biological systems. *Nature* 16:332–327.

Cumley RW, Crow A, Griffen B (1939). Clearing specimens for the demontration of bone. *Stain Technol.* 14:7-11.

Dodt H-U, Leischner U, Schierloh A, Jährling N, Mauch CP, Deininger K, et al. (2007). Ultramicroscopy: three-dimensional visualization of neuronal networks in the whole mouse brain. *Nat. Methods* 4:331–336.

Donati A, Domizi R, Damiani E, Adrario E, Pelaia P, Ince C (2013). From macrohemodynamic to the microcirculation (2013). *Crit Care Res Pract.*

Draenert K, Draenert Y (1980). The vascular system of bone marrow. *Scan Electron Microsc.*4:113–122.

Eberhard J, Loewen H, Kruger A, Donner S, Stumpp N, Patzlaff M, et al. (2014). Non-invasive in vivo imaging by confocal laser scanning microscopy of gingival tissues following natural plaque deposition. *J. Clin. Periodontol.* 41:321–326.

Egelberg JAN (1966). The blood vessels of the dento-gingival junction. *J. Periodontal*

Res.:163–179.

Erturk A, Becker K, Jahrling N, Mauch CP, Hojer CD, Egen JG, et al. (2012). Three-dimensional imaging of solvent-cleared organs using 3DISCO. *Nat Protoc* 7:1983–1995.

Fujimura A, Nozaka Y (2002). Analysis of the three-dimensional lymphatic architecture of the periodontal tissue using a new 3D reconstruction method. *Microsc. Res. Tech.* 56:60–65.

Grafström RC, Nymark P, Hongisto V, Spjuth O, Ceder R, Willighagen E, et al. (2015). Toward the replacement of animal experiments through the bioinformatics-driven analysis of "omics" data from human cell cultures. *Altern. Lab. Anim.* 43:325–332.

Griffini P, Smorenburg SM, Verbeek FJ, Van Noorden CJ (1997). Three-dimensional reconstruction of colon carcinoma metastases in liver. *J. Microsc.* 187:12–21.

Hama H, Kurokawa H, Kawano H, Ando R, Shimogori T, Noda H, et al. (2011). Scale: a chemical approach for fluorescence imaging and reconstruction of transparent mouse brain. *Nat. Neurosci.* 14:1481–1488.

Hira VVV, Ploegmakers KJ, Verbovšek U, Roing CS, Aronica EMA, Tigchelaar W, et al. (2015). CD133+ and nestin+ glioma stem-like cells reside around CD31+ arterioles in niches that express SDF-1α, CXCR4, osteopontin and cathepsin K. *J. Histochem. Cytochem.* 63:481–493.

Hoebe RA, Van Oven CH, Gadella TWJJ, Dhonukshe PB, Van Noorden CJF, Manders EMM (2007). Controlled light-exposure microscopy reduces photobleaching and phototoxicity in fluorescence live-cell imaging. *Nat. Biotechnol.* 25:249–253.

Icha J, Schmied C, Sidhaye J, Tomancak P, Preibisch S, Norden C (2016). Using light sheet fluorescence microscopy to image zebrafish eye development. 10(110).

Jalayeri Naderi N, Semyari H, Elahinia Z (2015). The impact of smoking on gingiva: a histopathological study. *Iran. J. Pathol.* 10:214–220.

Ke M-T, Fujimoto S, Imai T (2013). SeeDB : a simple and morphology-preserving optical clearing agent for neuronal circuit reconstruction. *Nat. Neurosci.* 16:1154–1161.

Keene JJ (1969). Observations of small blood vessels in human nondiabetic and diabetic gingiva. *J Dent Res.* 48:967.

Klaassen I, van Geest RJ, Kuiper EJ, van Noorden CJF, Schlingemann RO (2015). The role of CTGF in diabetic retinopathy. *Exp. Eye Res.* 133:37–48.

Kuwajima T, Sitko A, Bhansali P, Jurgens C, Guido W, Mason C (2013). ClearT: a detergent- and solvent-free clearing method for neuronal and non-neuronal tissue. *Development* 140:1364–1368.

Lee E, Choi J, Jo Y, Kim JY, Jang YJ, Lee HM, et al. (2016). ACT-PRESTO: Rapid and

consistent tissue clearing and labeling method for 3-dimensional (3D) imaging. *Sci. Rep.* 6:18631.

Lindhe J, Lang N, Karring T (2008). Clinical Periodontology and Implant Dentistry. Fifth edit. Blackwell, Munksgaard.

Matheny JL, Johnson DT, Roth GI (1993). Aging and microcirculatory dynamics in human gingiva. *J. Clin. Periodontol.* 20:471–475.

Matsuo M, Takahashi K (2002). Scanning electron microscopic observation of microvasculature in periodontium. *Microsc. Res. Tech.* 56:3–14.

Nuki K, Hock J (1975). The organisation of the gingival vasculature. *J. Periodontal Res.* 9:305.

Orban B (1948). Clinical and histologic study of the surface characteristics of the gingiva. *Oral Surg Oral Med Oral Pathol.* 1:827–841.

Parra SG, Vesuna SS, Murray TA, Levene MJ (2012). Multiphoton microscopy of cleared mouse brain expressing YFP. *J. Vis. Exp.*:e3848.

Peng H, Bria A, Zhou Z, Iannello G, Long F (2014). Extensible visualization and analysis for multidimensional images using Vaa3D. *Nat. Protoc.* 9:193–208.

Ramos de Carvalho JE, Verbraak FD, Aalders MC, Van Noorden CJ, Schlingemann RO (2014). Recent advances in ophthalmic molecular imaging. *Surv. Ophthalmol.* 59:393–413.

Renier N, Wu Z, Simon DJ, Yang J, Ariel P, Tessier-Lavigne M (2014). IDISCO: A simple, rapid method to immunolabel large tissue samples for volume imaging. *Cell* 159:896–910.

Retzepi M, Tonetti M, Donos N (2007). Comparison of gingival blood flow during healing of simplified papilla preservation and modified Widman flap surgery: a clinical trial using laser Doppler flowmetry. *J. Clin. Periodontol.* 34:903–911.

Schultz-Haudt SD, Paus S, Assev S (1961). Periodic acid-Schiff reactive components of human gingiva. *J Dent Res.* 40:141–147.

Söderholm G, Egelberg J (1973). Morphological changes in gingival blood vessels during developing gingivitis in dogs. *J Periodontol Res* 8:16–20.

Sorelli M, Bocchi L, Ince C (2015). Monitoring the microcirculation at the bedside using hand-held imaging microscopes: automatic tracking of erythrocytes. *Conf Proc IEEE Eng Med Biol Soc*:7378–7381.

Spalteholz W (1914). Über das Durchsichtigmachen von menschlichen und tierischen Präparaten und seine theoretischen Bedingungen, nebst Anhang. *S. Hirzel*.

Spalteholz W (1911). Über das Durchsichtigmachen von menschlichen und tierischen Präparaten, nebst Anhang: Über Knochenfärbung. *S. Hirzel*.

Steinke H, Wolff W (2001). A modified Spalteholz technique with preservation of the histology. *Ann. Anat.* 183:91–95.

Susaki EA, Tainaka K, Perrin D, Kishino F, Tawara T, Watanabe TM, et al. (2014). Whole-brain imaging with single-cell resolution using chemical cocktails and computational analysis. *Cell* 157:726–739.

Tomar SL, Asma S (2000). Smoking-attributable periodontitis in the United States: findings from NHANES III. National Health and Nutrition Examination Survey. *J. Periodontol.* 71:743–51.

Van Dyke T, Dave S (2005). Risk factors for periodontitis. *J Int Acad Periodontol.* 7:3–7.

Vesuna S, Torres R, Levene MJ (2011). Multiphoton fluorescence, second harmonic generation, and fluorescence lifetime imaging of whole cleared mouse organs. *J. Biomed. Opt.* 16:106009.

Weigelin B, Bakker G-J, Friedl P (2016). Third harmonic generation microscopy of cells and tissue organization. *J. Cell Sci.* 129:245–255.

Wesseling P, van der Laak JA, de Leeuw H, Ruiter DJ, Burger PC (1994). Quantitative immunohistological analysis of the microvasculature in untreated human glioblastoma multiforme. Computer-assisted image analysis of whole-tumor sections. *J. Neurosurg.* 81:902–9.

Wong TY, Cheung CM, Larsen M, Sharma S, Simo R (2016). Diabetic retinopathy. *Nat Rev Dis Prim.* 17.

Wu J, He Y, Yang Z, Guo C, Luo Q, Zhou W, et al. (2014). 3D Brain CV: Simultaneous visualization and analysis of cells and capillaries in a whole mouse brain with one-micron voxel resolution. *Neuroimage* 87:199–208.

Yang B, Treweek JB, Kulkarni RP, Deverman BE, Chen CK, Lubeck E, et al. (2014). Single-cell phenotyping within transparent intact tissue through whole-body clearing. *Cell* 158:945–958.

Figures:

Figure 1: Gingiva embedded in agarose before (A) and after clearing using BABB (B).

A

B

Figure 2: Low magnification 2D projection of a 3D image prepared with the use of light-sheet microscopy of human gingiva embedded in agarose with endothelium of blood vessels immunohistochemically stained using anti-CD31 antibodies conjugated with Alexa Fluor 568 (red) and nuclear staining using YOYO-3 (blue). Note that the colours are pseudocolours to optimize contrast.

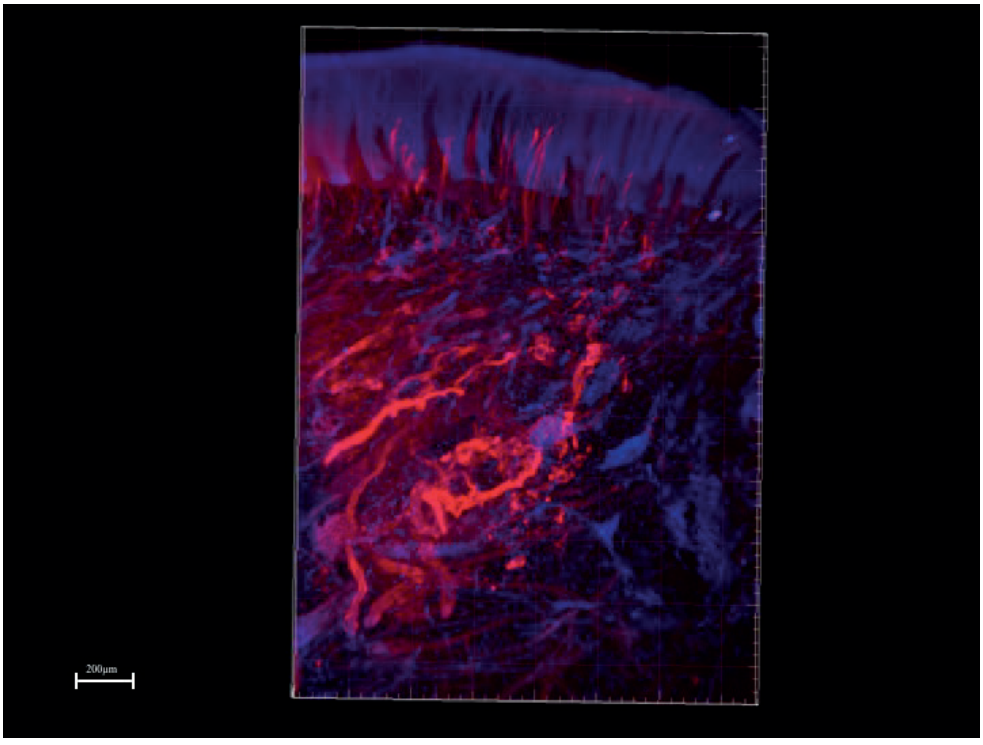

Figure 3: Higher magnification 2D projection of a 3D image prepared with the use of light-sheet microscopy of human gingiva embedded in agarose with endothelium of blood vessels immunohistochemically stained using anti-CD31 antibodies conjugated with Alexa Fluor 568 (red) and nuclear staining using YOYO-3 (blue). Note that the colours are pseudocolours to optimize contrast.

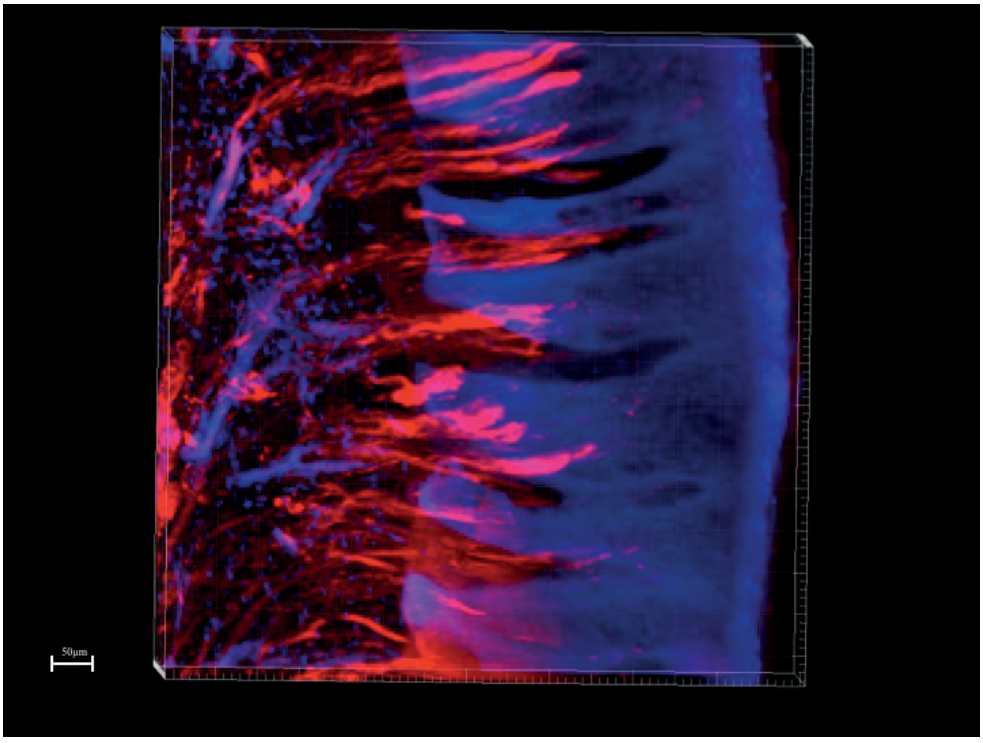

Figure 4: Detailed image of a capillary loop (red) in a papilla of the lamina propria of human gingiva taken from a larger 3D image obtained with the use of light-sheet microscopy